Wind and Structures, *Vol. 17, No. 3(2013) 263-274*
DOI:http://dx.doi.org/10.12989/was.2013.17.3.263

Numerical modelling for evaluating the TMD performance in an industrial chimney

A.L. Ibán[1], J.M.W. Brownjohn[2], A.V. Belver*[3], P.M. López-Reyes[3] and K. Koo[4]

[1]*ITAP, Escuela de Ingenierías Industriales, Universidad de Valladolid, Valladolid, 47011 Spain*
[2]*Vibration Engineering Section, University of Sheffield, Mappin Street, Sheffield S1 3JD, UK*
[3]*Centro Tecnológico CARTIF, Parque Tecnológico de Boecillo, Valladolid, 47151 Spain*
[4]*School of Construction Engineering, Kyoungil University, 712-701, Korea*

(Received June 14, 2012, Revised December 7, 2012, Accepted December 8, 2012)

Abstract. A numerical technique for fluid-structure interaction, which is based on the finite element method (FEM) and computational fluid dynamics (CFD), was developed for application to an industrial chimney equipped with a pendulum tuned mass damper (TMD). In order to solve the structural problem, a one-dimensional beam model (Navier-Bernoulli) was considered and, for the dynamical problem, the standard second-order Newmark method was used. Navier-Stokes equations for incompressible flow are solved in several horizontal planes to determine the pressure in the boundary of the corresponding cross-section of the chimney. Forces per unit length were obtained by integrating the pressure and are introduced in the structure using standard FEM interpolation techniques. For the fluid problem, a fractional step scheme based on a second order pressure splitting has been used. In each fluid plane, the displacements have been taken into account considering an Arbitrary Lagrangian Eulerian approach. The stabilization of convection and diffusion terms is achieved by means of quasi-static orthogonal subscales. For each period of time, the fluid problem was solved and the geometry of the mesh of each fluid plane is updated according to the structure displacements. Using this technique, along-wind and across-wind effects have been properly explained. The method was applied to an industrial chimney in three scenarios (with or without TMD and for different damping values) and for two wind speeds, showing different responses.

Keywords: finite element method; computational fluid dynamics; fluid-structure interaction; vortex shedding; damping

1. Introduction

The numerical technique presented in the work of Belver *et al*. 2012 and Belver *et al*. 2012 was applied to the particular chimney formerly located at Rugeley Power Station, England, UK. That chimney, now demolished, was constructed around 1968 and consisted of a 183 m high reinforced concrete windshield tapering from an external diameter of 9.4 m at the top to 15.7 m at the base (Fig. 1(a)).

*Corresponding author, Associate Professor, E-mail: alivas@cartif.es

http://www.techno-press.org/?journal=was&subpage=8 ISSN: 1226-6116 (Print), 1598-6225 (Online)

To study the wind-induced response of the chimney, a dynamic response monitoring system was installed, providing modal properties used for updating the structural finite element model. In its initial situation, the structural damping was very low ($\xi_1 \approx 0.7\%$), and this was increased when the chimney was equipped with a tuned mass damper (TMD) adjusted to the first natural frequency. The TMD, located at 16 m from the top and described in the work of Brownjohn *et al*. (2010), comprised 42 tons of pendular moving mass (hollow steel ring filled with concrete) hung by several cables and with five viscous damper units, with a 0.45 m stroke (Fig. 1(b)).

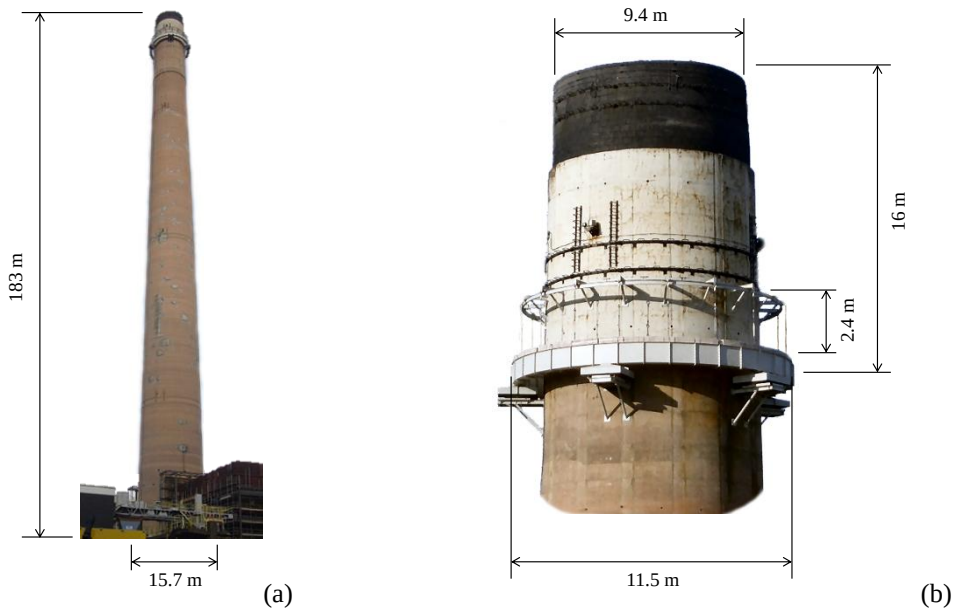

Fig. 1 Description of the chimney and TMD

Table 1 Chimney data

Property	Value
E	24720 MPa
ρ	2436 Kg/m^3
First natural freq. (n_{e1})	0.338 Hz
Second natural freq. (n_{e2})	1.4 Hz
Foundation stiffness	8110 MN/m^2
Modal mass (unit at TMD location)	$1.28 \cdot 10^6$ kg
Poison ratio	0.2
Damping ratio (ξ)	0.7 %

The damping of the combined chimney plus TMD system increased to around $\xi_2 = 2.5\%$, occasionally even higher. When this damping was considered in the initial model of the chimney (the updated one without TMD, just changing ξ_1 for ξ_2), the shape and amplitude of the numerical orbit plots were different from the recorded ones for similar winds. Using a more sophisticated

numerical model, in which the chimney was considered with ξ_1 and the TMD device was properly included in the FEM model, computed orbit plots agree with the experimental ones, not only in amplitude but also in shape. Numerical simulations are used here to compare response of these three models (or scenarios) for two different wind speeds.

Using information from previous studies (Brownjohn *et al*. 2010, Brownjohn *et al*. 2009), there was sufficient information to make an updated finite element model for the chimney under study. The data used are listed in Table 1.

The values of mass ratio, stiffness and damping as well as the resulting first mode natural frequencies for the assembly are listed in Table 2. Note that the initial value for n_{e1} = 0.338 Hz in the bare chimney is decoupled by the TMD into n_{e1}^{L} = 0.305 Hz and n_{e1}^{R} = 0.370 Hz.

.

Table 2 Characteristics of the chimney with the TMD

Property	Value
Mass ratio	3.27 %
Equivalent stiffness	180 kN/m
Damping coefficient	18 kNs/m
Frequency n_{e1}^{L}	0.305 Hz
Frequency n_{e1}^{R}	0.370 Hz

The monitoring system carried out real time operational modal analysis, estimating the modal frequencies and damping ratios using the stochastic subspace identification (SSI) algorithm (Brownjohn *et al*. 2010, Magalhães *et al*. 2010). The trend of damping ratios over long term is presented in Fig. 2. The period 'before TMD' in fact represents the long period during which the TMD was constructed and before it became operational.

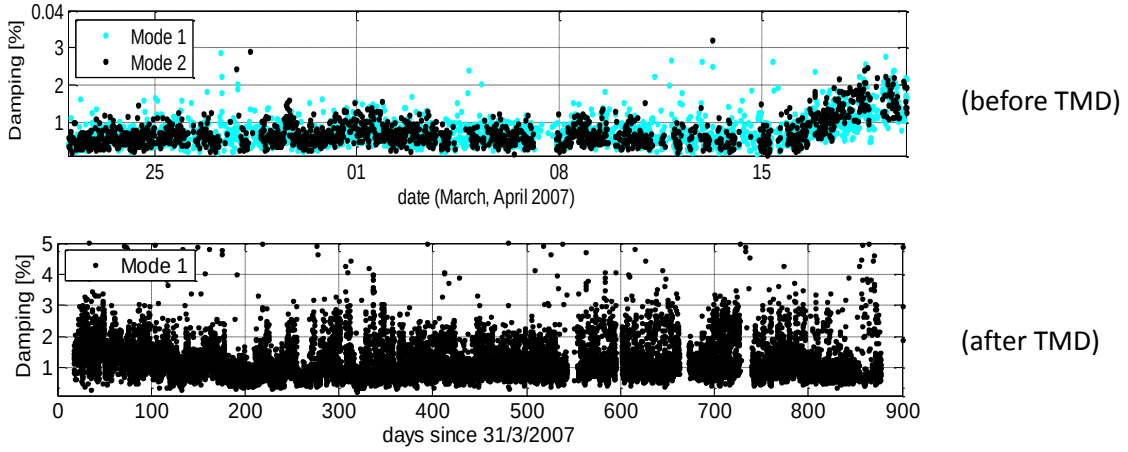

Fig. 2 Damping estimates before and after TMD installation (Brownjohn *et al*. 2010)

The TMD attached to the chimney is in fact a non-linear system. Both load and structural system were non-stationary, so a wide range of damping ratios were identified while the TMD was in operation. Nonlinear and varying performance of the structure itself could derive from the behaviour of the old cracked concrete, effects of internal and external temperature on expansion and contraction as well as directly on the material properties. The greatest nonlinearity would likely be due to the behaviour of the damping fluid used in the TMD which results in velocity-dependent damping, but there could be other factors involved, as aerodynamic effect or large displacements. In fact, the TMD was installed in order to mitigate interference effects on the old chimney due to the construction of a new one at 110 m distance. Nevertheless, a mean value of 0.7% was taken as representative for the chimney without TMD and 2.5% with TMD.

The purpose of this study was to determine whether or not numerical simulation can explain the structural behaviour registered, using three different finite element models: the chimney without the TMD and with 0.7% structural damping, the chimney with the TMD in such a way that the structural damping of the assembly was 2.5% and finally the chimney without the TMD but with 2.5% structural damping. Numerical simulations are presented to compare the response of these three models (or scenarios) for two different wind speeds (v_{10}^1 and v_{10}^2) including, when possible, a comparison between numerical accelerations and corresponding observed response.

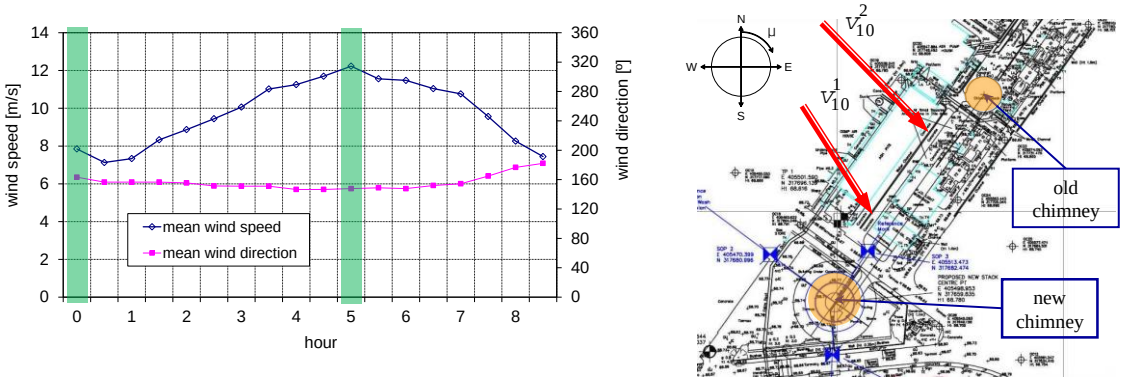

Fig. 3 Wind data and layout showing selected wind directions

2. Modelling

Among the available meteorological data and experimental recorded acceleration response, two specific wind speeds were selected for the study, v_{10}^1 = 7.8 m/s and v_{10}^2 = 12.2 m/s, for a particular windy day (2008/03/10) where the directions were out of the range where interference phenomena due to the new chimney could appear. These speeds can be considered approximately constant in the considered time range (shaded area in Fig. 3, around 0:00 h for v_{10}^1 and 5:00 h for v_{10}^2), consistent with the requirements of the numerical simulation technique. As discussed below, for those speeds, the resulting behaviours are substantially different. Corresponding bearing angles were 163° and 147° (0 degree starting from North, clockwise direction), being the angle between

chimneys 218º. The layout is shown in Fig. 3 where the arrows indicate the wind direction for v_{10}^1 and v_{10}^2.

In the numerical approach, the wind was not modelled in the whole volume. For particular fluid-structure interaction problems, where the main flow is considered to act in the transversal direction of the slender structure, the effects of the 3D flow around the structure can be approximated by the effects of several 2D flows around the cross section of the structure (Nieto *et al*. 2010). In this case, the effects of the wind on the chimney are evaluated, according to former convergence studies (Belver *et al*. 2010, Belver *et al*. 2010, Vasallo *et al*. 2009) in just two fluid planes, one located at the tip (denoted as _1) and the other at 2/3 of the height (denoted as _2) (Fig. 4).

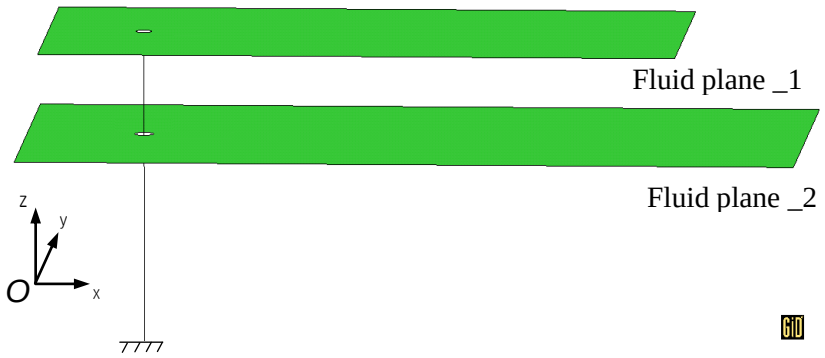

Fig. 4 Model of old chimney with two fluid planes

The chimney was meshed just with 12 beam elements but more than 30.000 triangular fluid elements are necessary for both planes. The size of the mesh around the boundary of the circular cross section was around 0.05 times the corresponding diameter (9.4 m). This small size was demanded by the CFD algorithm and leads to the necessity of updating the mesh at specific time intervals.

The solution on each fluid plane provides the transversal forces acting on the cross-section of the beam. These forces (in the along- and across- wind directions) were obtained by integrating the pressure of the fluid over the corresponding boundary. A time-varying distributed load over the beam was obtained by linear interpolation between consecutive fluid planes. Note that the simplified approach adopted only is able to account for transversal effects. Effects in the longitudinal direction, including complex flow around the tip, were neglected.

With the focus on the transversal behaviour of the chimney, both planes are considered representative of the vortex shedding phenomenon that can occur in the whole chimney (Armitt 1969, Vickery and Clark 1972, Williamson and Govardhan 2008, Flaga and Lipecki 2010). It is important to have in mind that the response of the chimney is also affected by two wind effects related to vortex shedding, the first being the lock-in effect (Belver *et al*. 2012, Adaramola *et al*. 2009). Although the Strouhal law predicts a linear relationship between wind speed and vortex shedding frequency, for slender structures there is a range, around fundamental frequency, where

the shedding frequency is not the predicted by Strouhal number, but just the fundamental frequency of the structure. The other effect is that vortices are volumetric phenomena, organized in cells (Vickery and Clark 1972, Hsiao *et al*. 1998, Ruscheweyh 2009) in such a way that although for every wind speed and cross-section diameter of the chimney the shedding frequency should be different, according to Strouhal law; in fact, just a few different frequencies appear. Considering these two effects in analytical or semi-empirical formulations is not so simple, whereas in the numerical approach they are intrinsically included. In fact, according to the "cell-effect" the simplified CFD approach adopted makes sense, although obviously some vertical and tip effects are lost. Nevertheless, using that approach it is possible to obtain qualitative as well as quantitative results, as shown in this paper.

In each fluid plane, the frequency of the vortex shedding was determined by post-processing CFD results (Table 3). Note that those frequencies are different because wind speeds and diameters both vary with height. A standard speed distribution with height (Simiu and Scanlan 1996) was considered: $v(h)=v_{10}(h/10)^{0.154}$, and the Strouhal number, *St*, was evaluated using the formula $St=n_s*d/v$.

Table 3 Vortex shedding frequency in each fluid plane

	Height [m]	Diameter, *d* [m]	Velocity, *v* [m/s]	Vortex shedding frequency, n_s [Hz]	*St*
v_{10}^1 = 7.8 m/s	183.88 (_1)	9.4	12.21	0.278	0.214
	122.92 (_2)	11.5	11.48	0.217	0.217
v_{10}^2 = 12.2 m/s	183.88 (_1)	9.4	19.10	0.44	0.216
	122.92 (_2)	11.5	17.95	0.34	0.218

The pressure field at two representative instants for the considered cases for scenario 1 is shown in Figs. 5(a) and 5(b).

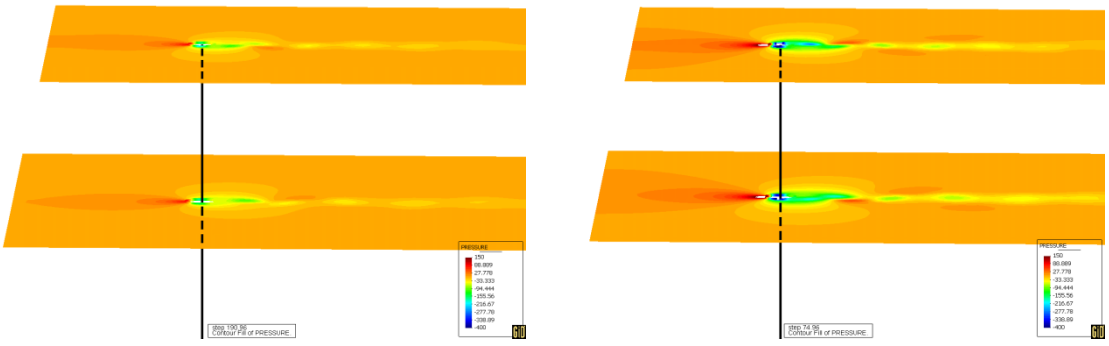

(a) (b)

Fig. 5 Field pressure for (a) v_{10}^1 = 7.8 m/s and (b) v_{10}^2 = 12.2 m/s

The three scenarios to be discussed are:

(a) chimney before the installation of TMD. The data for the finite element model is the one collected in Table 1, for a damping of 0.7%, with first natural frequency 0.338 Hz

(b) chimney (a) but equipped with the TMD (Casado *et al*. 2007) according to the data of Table 2. First natural frequencies are 0.305 Hz and 0.370 Hz, although the higher mode frequency was not observed in the monitoring data.

(c) similar chimney to (a) but with a damping of 2.5%. Note that this is the total value of damping considered for the combined system (b). Because of that, this scenario is denoted as "equivalent" (EQ) to (b), but also in damping, not in frequencies (its first natural frequency remains 0.338 Hz)

3. Results

Time loading plots for scenario 1 for the 2 planes (_1 and _2) and their power spectral density plots (PSD) are shown in the Figs. 6 and 7, both in along-wind (X) and across-wind (Y) directions. Note that in the plane at the tip, although the speed is higher, the drag force (per unit length), F_x is less than in the second plane because the stack diameter in the second plane is larger in the tapered chimney. Nevertheless, in the across-wind direction (lift), force amplitudes, F_y are higher at the tip (_1) than at 2/3 (_2)

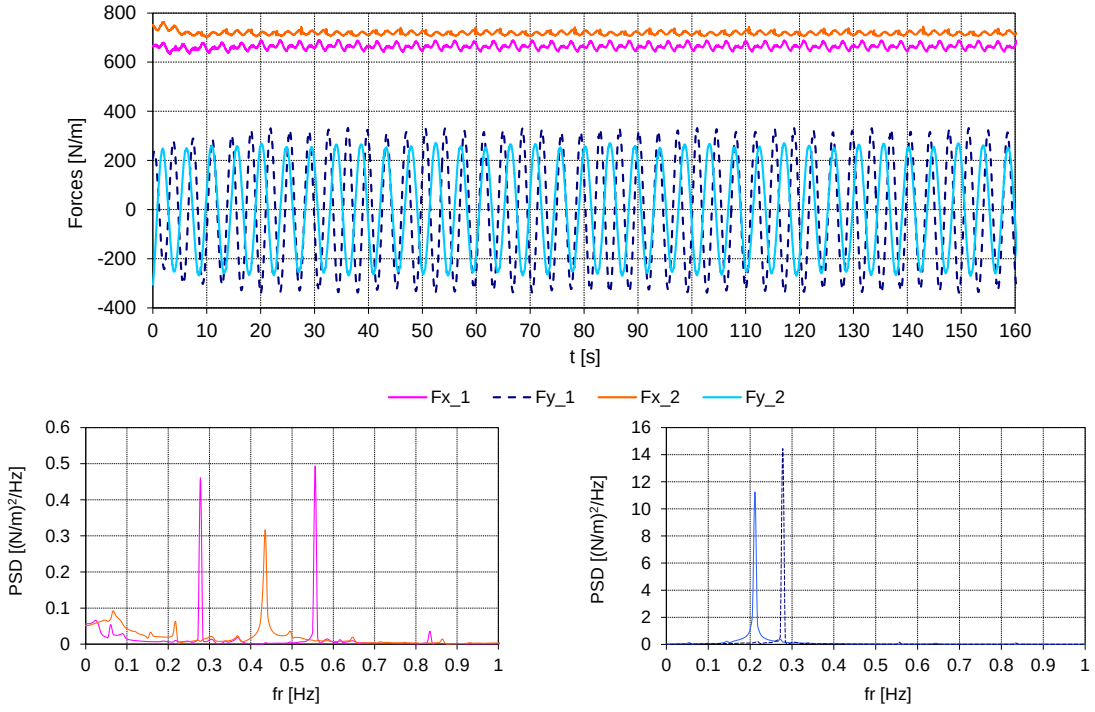

Fig. 6 Forces and PSD in along-wind (F_x) and across-wind (F_y) for v_{10}^1 = 7.8 m/s

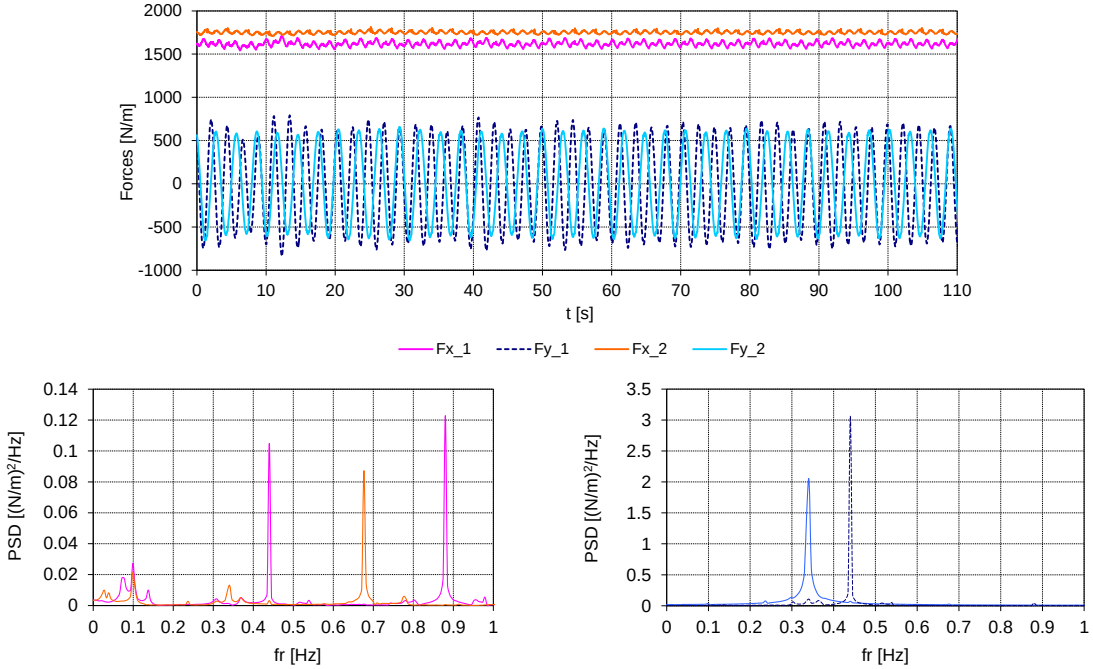

Fig. 7 Forces and PSD in along-wind (F_x) and across-wind (F_y) for v_{10}^2 = 12.2 m/s

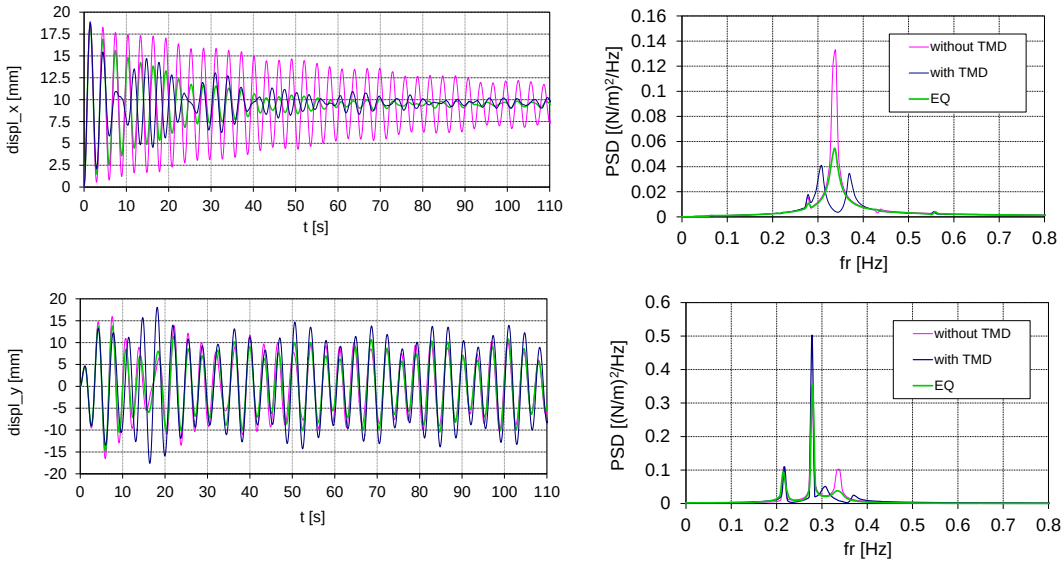

Fig. 8 Time history across- and along-wind displacements for v_{10}^1 = 7.8 m/s

These forces are supposed to act over the chimney in the following way: at time t = 0 s the

chimney is assumed to be at rest and at that time both F_x and F_y forces are apply suddenly. In this way, it is possible to check, in the along-wind direction, the damping using a standard free decay curve-fitting approach. Also, it is possible evaluate the performance of the TMD in the along-wind and across-wind direction and the damping ratios using the SSI algorithm. Responses for the three scenarios are shown in Figs. 8 and 9. Because the along wind force includes a suddenly applied DC component the response has a strong transient component.

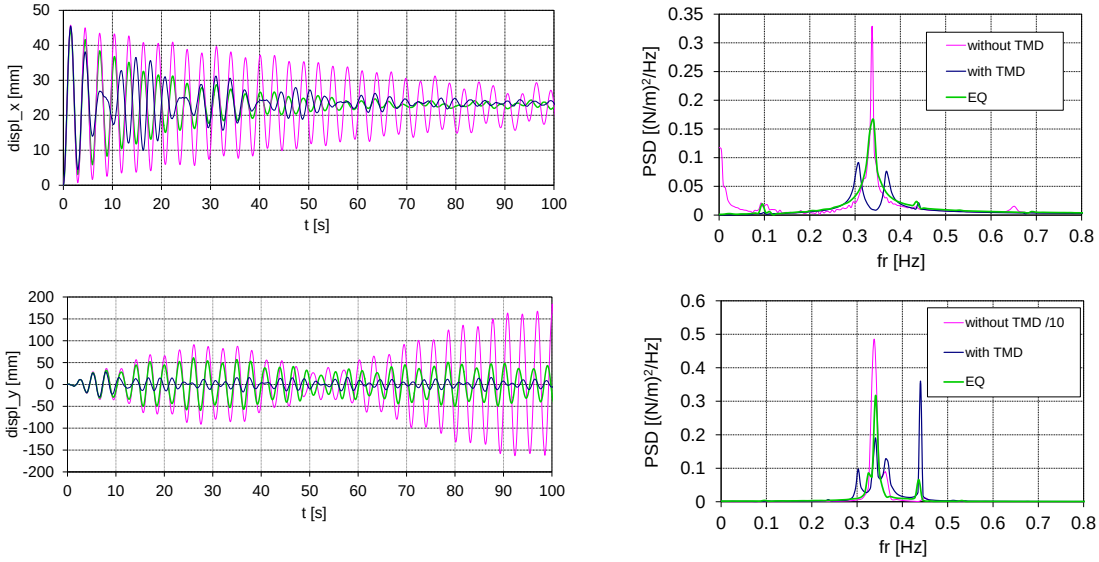

Fig. 9 Time history across- and along-wind displacements for v_{10}^2 = 12.2 m/s

In both cases, the TMD is successfully working in the along-wind direction. Nevertheless, in the across-wind direction the performance is very different, even accounting for the transient in the along wind response. For the wind velocity v_{10}^1, the force amplitude and the frequency of the vortex shedding are insufficient to force the chimney at appropriate frequencies to which TMD is tuned. However for wind velocity, v_{10}^2, the chimney is excited differently (in amplitude and, mainly, in frequencies) in such a way that the TMD behaves very efficiently. Fig. 9 also shows that, in this case, the equivalent scenario is not equivalent at all from the kinematic point of view.

Also, in Fig. 10, numerical displacement orbit plots are shown for the three considered scenarios. The same time spans ($142 < t < 160$ s for v_{10}^1 = 7.8 m/s and $75 < t < 93$ s for v_{10}^2 = 12.2 m/s) are taken.

Comparing the differences in the behaviour provides interesting observations. Without the TMD, the across-wind response for the wind velocity, v_{10}^2, is ten times larger than for the wind velocity, v_{10}^1, whereas with the TMD the responses are similar due to TMD working for the wind velocity, v_{10}^2. The shedding frequency for v_{10}^2 is in the range where TMD is tuned whereas for v_{10}^1 is not. For the wind velocity v_{10}^1 the three scenarios present similar amplitudes whereas for

the wind velocity, v_{10}^2, amplitudes without TMD are 7 times bigger than with TMD and 1.7 times bigger than for the model with equivalent damping.

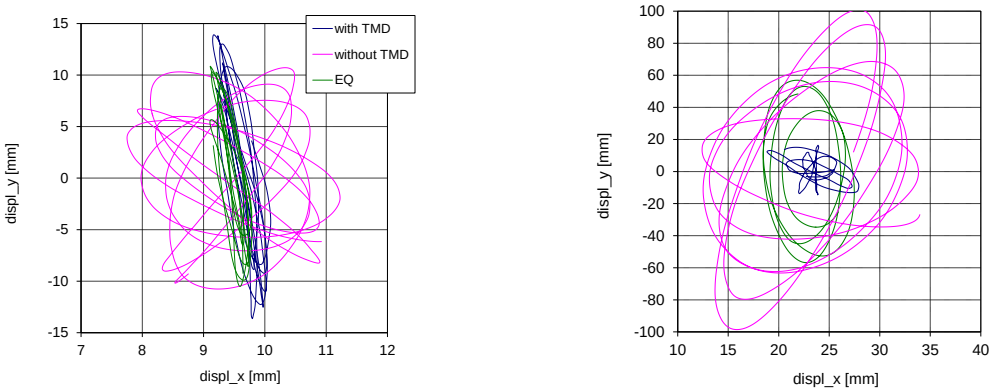

(a) (b)

Fig. 10 Displacement orbit plots for (a) v_{10}^1 = 7.8 m/s and (b) v_{10}^2 = 12.2 m/s

In order to validate the results, experimental and numerical acceleration orbit plots are compared in Fig. 11. The numerical orbits are taken from the simulation (case (b) with TMD) between t = 142 s and 160 s (v_{10}^1) and t = 75 s and 93 s (v_{10}^2). The experimental orbits are from 2008/03/10 at the time 0 h 42 min and 5 h 53 min, respectively. Note that experimental acceleration data are only available for the chimney with the TMD and for this case, for each speed, experimental and numerical acceleration orbit plots exhibit similar amplitudes in both directions.

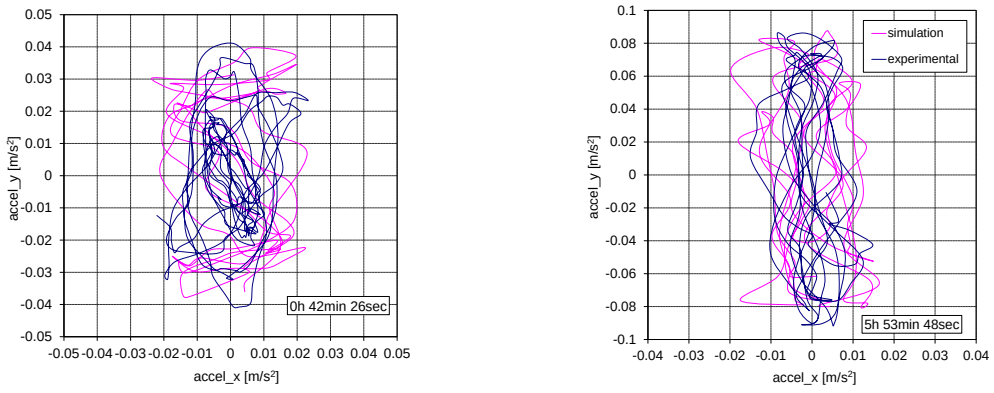

(a) (b)

Fig. 11 Acceleration orbit plots for (a) v_{10}^1 = 7.8 m/s and (b) v_{10}^2 = 12.2 m/s

4. Conclusions

A simplified numerical method for evaluation of vortex induced vibrations in line-like slender structures has been evaluated using a full-scale 183 m chimney equipped with a TMD. The observed response of the chimney was different depending on the damping and on the wind speed.

Three different finite element models were considered. In the first scenario, the chimney was considered to be a structure without TMD. This model was appropriate for the initial conditions of the chimney, for which the damping was very low (0.7%).

Once installed and operational, the TMD increased the equivalent measured damping of the assembly to 2.5%, except during calm conditions when the TMD was not engaged. For the second scenario, the chimney was modelled as in previous scenario, but the TMD device was properly included in the model as an assembly of the chimney structure stack with the moving mass having the corresponding concentrated damping coefficient. The third scenario is similar to the first one (no assembly) but with more structural damping. Responses of these three models under similar winds were very different, not only between the first scenario and the other two, but also between second and third ones, revealing that they were not equivalent, as intended. For the case where experimental results are available, amplitudes were similar so the numerical method was considered to be validated.

This kind of study shows that it is possible to simulate, using proper simplified numerical techniques, the performance of TMD devices installed in civil structures under wind actions.

Acknowledgments

Authors wish to acknowledge to the International Committee on Industrial Chimneys (CICIND) for its technical and financial support. Also the support of Research Project BIA2011-28493-C02-02 ("Ministerio de Economía y Competitividad", Spanish Government) is acknowledged.

References

Armitt, J. (1969), *Wind-excited vibration of chimneys*, Leatherhead, Surrey RD/L/N 89/69.

Adaramola, M.S. Sumner, D. and Bergstrom, D.J. (2009), "Effect of velocity ratio on the streamwise vortex structures in the wake of a stack", *J. Fluids. Struct.*, **14**(1), 477-486.

Belver, A.V., Ibán, A.L. and Foces, A. (2010), *Analysis of aero elastic vibrations in slender Structures subjected to Wind Action, 73rd CICIND Technical Meeting*, CICIND REPORT. International Committee on Industrial Chimneys.

Belver, A.V., Ibán, A.L. and Martín, C.E.L. (2012), "Coupling between structural and fluid dynamic problems applied to vortex shedding in a 90 m steel chimney", *J. Wind Eng. Ind. Aerod.*, **100**(1), 30-37.

Belver, A.V., Mediavilla, A.F., Iban, A.L. and Rossi, R. (2010), "Fluid-structure coupling analysis and simulation of a slender composite beam", *Sci. Eng. Compos. Mater.*, **17**(1), 47-77.

Belver, A.V., Rossi. R. and Iban, A.L. (2012), "Lock-in and drag amplification effects in slender line-like structures through CFD", *Wind Struct.*, **15**(3), 189-208.

Brownjohn, J.M.W., Carden, E.P., Goddard, R.C. and Oudin, G. (2010), "Real-time performance monitoring of tuned mass damper system for a 183m reinforced concrete chimney", *J. Wind Eng. Ind. Aerod.*, **98**, 169-179.

Brownjohn, J.M.W., Carden, E.P., Goddard, R.C., Oudin, G. and Koo, K. (2009), "Real-time performance tracking on a 183m concrete chimney and tuned mass damper system", *Proceedings of the IOMAC09, 3rd International Operational Modal Analysis Conference*.

Casado, C.M., Poncela, A. and Lorenzana, A. (2007), "Adaptive tuned mass damper for the construction of concrete pier", *J. Struct. Eng. - ASCE*, **17**(3), 252-255.

Flaga, A. and Lipecki, T. (2010), "Code approaches to vortex shedding and own model", *Eng. Struct.*, **32**(6), 1530-1536.

Hsiao, F.B. and Chiang, C.H. (1998), "Experimental study of cellular shedding vortices behind a tapered circular cylinder", *Exp. Therm. Fluid Sci*., **17**(3), 179-188.

Magalhãesa, F., Cunhaa, A., Caetanoa, E. and Brinckerb, R. (2010), "Damping estimation using free decays and ambient vibration tests", *Mech. Syst. Signal. Pr.*, **24**(5), 1274-1290

Nieto, F., Hernández, S., Jurado, J.A. and Baldomir. (2010), "CFD practical application in conceptual design of a 425 m cable-stayed bridge", *Wind Struct.*, **13**(4), 309-326.

Ruscheweyh, H. (2009), *Experience with vortex-induced vibrations, CICIND international committee on industrial chimneys*, Technical Report.

Simiu, E. and Scanlan, R. (1996), *Wind Effects on Structures*, 3rd Ed., John Wiley and Sons.

Vasallo, A., Lorenzana, A., Foces, A. and Lavín, C.E. (2009),"Simplified numerical method for understanding the aeroelastic response of line slender structures under vortex shedding action", *Proceedings of the 5th International Conference on Fluid Structure Interaction*, Fluid structure interaction.

Vickery, B.J. and Clark, A.W. (1972), "Lift or across-wind response of tapered stacks", *J. Struct. Div.*, **98**, 1-20.

Williamson, C.H.K. and Govardhan, R. (2008), "A brief review of recent results in vortex induced vibrations", *J. Wind Eng. Ind. Aerod.*, **96**(6-7), 713-735.

JH